Supplemental Material for "Giant topological insulator gap in graphene with 5d adatoms"

Jun Hu,[1] Jason Alicea,[1,2,*] Ruqian Wu,[1,†] and Marcel Franz[3]

[1]*Department of Physics and Astronomy, University of California, Irvine, California 92697*
[2]*Department of Physics, California Institute of Technology, Pasadena, California 91125*
[3]*Department of Physics and Astronomy, University of British Columbia, Vancouver, BC, Canada V6T 1Z1*

PACS numbers:

EVALUATION OF THE Z_2 INVARIANT

The tight-binding model studied in the main text preserves (three-dimensional) inversion symmetry about an adatom site, which sends $c_{\mathbf{r}\alpha} \to c_{-\mathbf{r}\alpha}$ and $f_{m\mathbf{R}\alpha} \to -f_{m-\mathbf{R}\alpha}$. Thus one can simultaneously diagonalize the Hamiltonian and the operator $\mathcal{R}$ implementing this transformation. Fu and Kane [1] showed that the Z_2 invariant can be deduced very simply from the inversion eigenvalues of energy eigenstates at the four time-reversal-invariant momenta $\mathbf{P}_j$ that satisfy $\mathbf{P}_j = -\mathbf{P}_j$ up to a reciprocal lattice vector. For the 4×4 supercell considered in the main text these momenta are $\mathbf{P}_1 = (0,0)$ at the zone center and $\mathbf{P}_2 = (0, \frac{\pi}{2\sqrt{3}})$, $\mathbf{P}_3 = (\frac{\pi}{4}, \frac{\pi}{4\sqrt{3}})$, and $\mathbf{P}_4 = (\frac{\pi}{4}, -\frac{\pi}{4\sqrt{3}})$ at the midpoints of the zone edges (here we have set the lattice constant to unity).

Suppose that there are $2N$ fully occupied bands, enumerated such that bands $2m-1$ and $2m$ are Kramer's partners that thus transform in the same way under $\mathcal{R}$. Let $\xi_{2m}(\mathbf{P}_j)$ be the inversion eigenvalue for band $2m$ at time-reversal-invariant momentum $\mathbf{P}_j$. Fu and Kane's Z_2 invariant ν then follows from

$$(-1)^\nu = \prod_{j=1}^{4} \prod_{m=1}^{N} \xi_{2m}(\mathbf{P}_j). \qquad (1)$$

Trivial insulating states are characterized by $\nu = 0$ while $\nu = 1$ indicates a topological phase. By diagonalizing our tight-binding model with periodic boundary conditions it is straightforward to numerically extract $\xi_{2m}(\mathbf{P}_j)$ for all m and j and hence evaluate the topological invariant for an insulating state using Eq. (1). Carrying out this procedure we find that the spin-orbit-induced insulating phase discussed in the main text is indeed topological, consistent with our identification of edge states in numerical simulations of systems with open boundaries.

As an interesting aside, we remark that Fig. 1(c) in the main text shows that spin-orbit coupling actually opens *three* different insulating regimes. One can use the above criterion to show that all of these are in fact topologically non-trivial. This suggests that many if not all of the insulating regimes present in our density functional theory simulations are also topological, though most of these are not expected to be relevant physically since they require very large dopings to access.

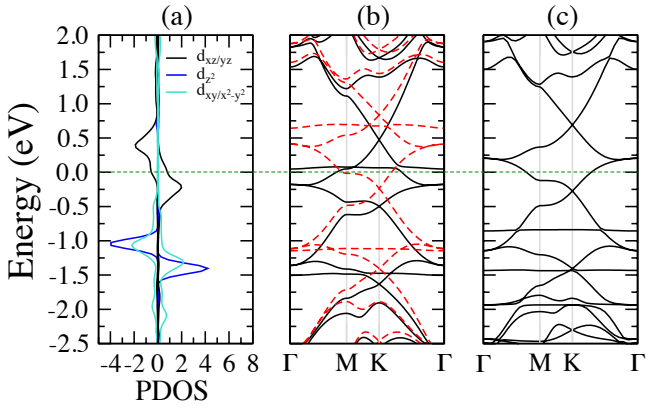

FIG. 1: Electronic properties of Os/graphene and (Cu-Os)/graphene at 6.25% coverage *without* spin-orbit coupling. (a) Partial density of states (PDOS) for the Os $5d$ orbitals in Os/graphene. Positive and negative values on the horizontal axis correspond to the PDOS for the spin majority and minority channels, respectively. The horizontal dashed lines indicate the Fermi level. (b) Band structure for Os/graphene. The solid and dashed lines respectively indicate majority and minority spin bands, which are widely separated due to strong moment formation in the non-relativistic limit. (d) Band structure of (Cu-Os)/graphene. In both (b) and (c) the spectrum is always metallic, demonstrating that the gaps found earlier indeed originate from spin-orbit coupling.

DENSITY FUNCTIONAL THEORY METHODS

In our DFT simulations the positions of all atoms were fully relaxed using the conjugated gradient method for energy minimization until the calculated force on each atom became smaller than 0.01 eV/Å. We used the projector augmented wave (PAW) method for the description of the core-valence interactions [2, 3]. A vacuum space of 15 Å was adopted to separate the periodic graphene slabs. The two-dimensional Brillouin zone was sampled by a 15×15 k-grid mesh [4]. The energy cutoff of the plane wave expansion was set to 500 eV.

ELECTRONIC PROPERTIES WITHOUT SPIN-ORBIT COUPLING

To confirm that the band gaps induced by Os and Cu-Os stem from spin-orbit coupling, we performed DFT calculations for these adatoms at 6.25% coverage in the non-

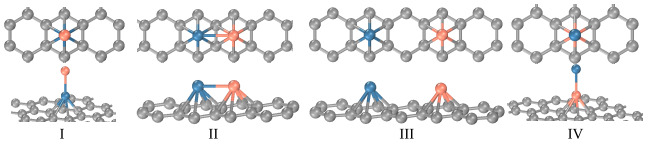

FIG. 2: Different configurations for Cu-Os co-adsorption. The dark cyan, coral, and gray spheres represent Os, Cu, and C atoms, respectively.

relativistic limit. For Os/graphene, we find that in the absence of spin-orbit coupling the Os spins polarize much more strongly compared to the relativistic case yielding a magnetic moment $M_s = 1.52\mu_B$ which is close to the generalized gradient approximation (GGA) result in a recent paper ($M_s \approx 1.3\ \mu_B$) [5]. The spin splitting is clearly visible in the partial density of states for the Os $5d$ orbitals shown in Fig. 1(a), where positive and negative values on the horizontal axis correspond respectively to the majority and minority spin channels. The band structure for the majority spins (solid curves) and minority spins (dashed curves) appears in Fig. 1(b). Notice that in sharp contrast to the spin-orbit-coupled case, both spin channels are always gapless for any value of the chemical potential (at least over the energy range shown). Interestingly, (Cu-Os)/graphene remains non-magnetic even in the absence of spin-orbit coupling. From the band structure in Fig. 1(c) one clearly sees that here, too, the system remains gapless in the non-relativistic limit. Thus for both Os/graphene and (Cu-Os)/graphene the gaps indeed originate solely from spin-orbit interactions.

ENERGIES OF DIFFERENT Cu − Os CO-ADSORPTION CONFIGURATIONS

In the main text we remarked that Cu and Os co-adsorbates energetically prefer to form vertical dimers over the H-site in graphene. Here we summarize the evidence supporting this conclusion. We used DFT, without spin-orbit coupling, to explore the energetics of the various configurations displayed in Fig. 2 (Os, Cu, and C atoms are respectively represented by dark cyan, coral, and gray spheres). Note that in all cases we fix the Os to the H-site since the binding energy for that position greatly exceeds that for the top or bridge sites. (Additionally, Cu-Os dimers bind much more weakly to the top and bridge positions.) The vertical Cu-Os dimer in configuration I exhibits a very large binding energy $E_b = 6.17$ eV. In contrast the binding energy for configurations III and IV are substantially lower by 2.50 and 2.09 eV, respectively. Configuration II is unstable and transforms to configuration I after relaxation, indicating a strong tendency toward vertical dimer formation. Incidentally, this is why no intermediate points between A and B are shown in Fig. 4(d) of the main text. As we saw earlier the vertical dimer in (a) is nonmagnetic (with or without spin-orbit coupling), whereas the other configurations are magnetic.

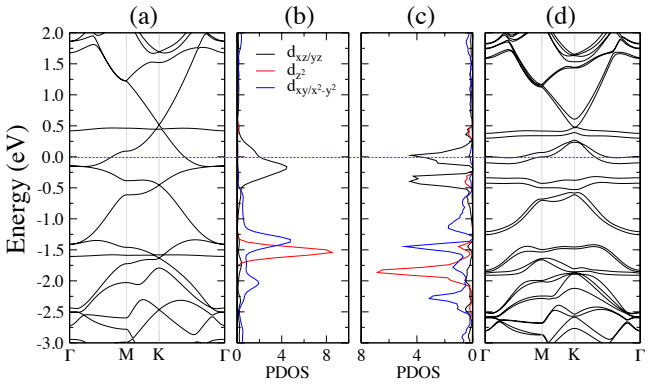

FIG. 3: (a) Band structure and (b) PDOS for Ir 5d orbitals obtained for Ir/graphene at 6.25% coverage, *without* SOC. The green horizontal dashed line denotes the Fermi level. Here the system is nonmagnetic, and the spectrum is again always gapless similar to Figs. 1(b) and (c). In (c) and (d) we display the PDOS and band structure calculated with spin-orbit coupling. A large spin-orbit-induced gap opens below the Fermi level, though the bands are split slightly due to weak moments formed by Ir in this case. As discussed in the main text replacing Ir with Cu-Ir dimers returns the Fermi level to within the gap *and* quenches the moment to restore time-reversal symmetry.

We would also like to comment here on our calculation of the Cu diffusion barrier described in the main text. The energies for various positions along the trajectory in Fig. 4(c) of the main text were computed without spin-orbit coupling. The system's energy is not expected to change significantly, however, with the inclusion of relativistic effects since Cu exhibits relatively weak spin-orbit interactions. Note also that since Cu is physisorbed on graphene, changes to the diffusion trajectory examined there will not appreciably alter the diffusion barrier.

RESULTS FOR Ir/GRAPHENE

Here we briefly highlight our results for Ir adatoms on graphene. We found that Ir slightly prefers the H site over the bridge site, the binding energy being 2.17 eV in the former configuration and 2.12 eV in the latter. The binding energy for Ir at the top site is weakest at 1.94 eV. All results discussed henceforth thus correspond to H-site Ir adatoms. Without spin-orbit coupling DFT predicts that Ir/graphene is non-magnetic. Figures 3(a) and (b) illustrate the band structure and partial density of states for the Ir $5d$ levels, calculated at 6.25% coverage. Just as for Os and Cu-Os dimers, here too the system remains gapless in the non-relativistic limit.

Figure 3(d) shows that restoring spin-orbit coupling introduces a huge band gap $\Delta_{SO} = 0.21$ eV below the Fermi level (green dashed line). Moreover, in Fig. 3(c) we see that this gap results from hybridization between the Ir $d_{xz/yz}$ orbitals and graphene's π bands, similar to Os/graphene and the tight-binding model described in the main text. Spin-orbit interactions also, however, produce small spin and orbital moments

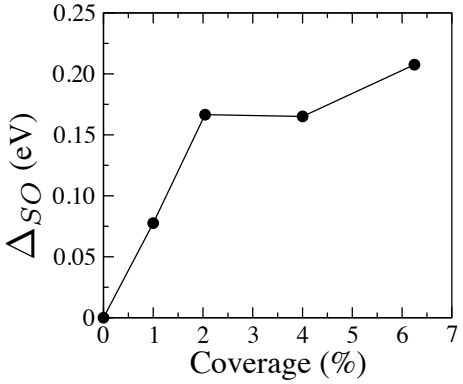

FIG. 4: Spin-orbit-induced band gap of Ir/graphene as a function of Ir coverage. Data were obtained using 4×4, 5×5, 7×7 and 10×10 graphene supercells that contain one Ir adatom over the H site.

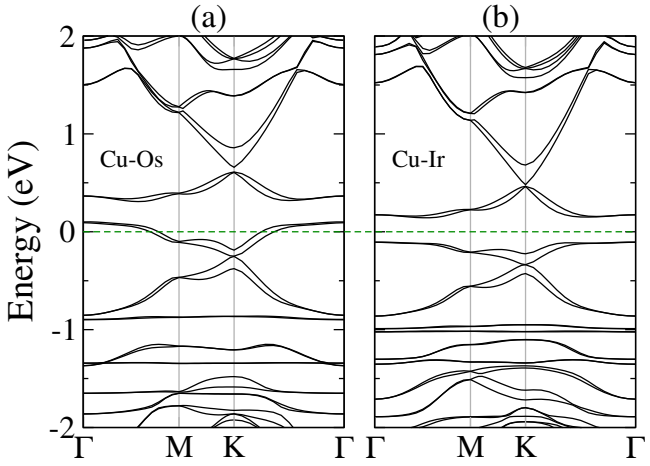

FIG. 5: GGA band structures of (a) (Cu-Os)/graphene and (b) (Cu-Ir)/graphene at 6.25% coverage with spin-orbit coupling. The green dashed line indicates the Fermi energy.

for Ir given respectively by 0.30 μ_B and 0.13 μ_B; these are responsible for the weak band splittings in Fig. 3(d). Coverage dependence of the gap is illustrated in Fig. 4. As in all other cases studied here, the gap remains quite large down to very dilute Ir concentrations. Even at 1% coverage where Δ_{SO} reduces to 0.08 eV the gap exceeds that induced by In or Tl adatoms [6] many times over.

Observing a true topological insulator phase in Ir/graphene is complicated by the magnetic moments predicted by DFT and the fact that the Fermi level resides in the conduction band. (One should again keep in mind, however, that DFT may overestimate the tendency for moment formation here. Furthermore, it may be feasible to gate the system back to the insulating regime by conventional means at low coverages.) In the main text we described how co-doping with Cu eliminates both potential challenges. Here we simply wish to note that Cu-Ir dimers carry yet another advantage—they strongly enhance binding to the H-site compared to isolated Ir adatoms, similar to the Os case. Indeed, the binding energy for Cu-Ir dimers over the H-site is larger by 0.62 eV and 0.79 eV compared to the bridge and top sites, respectively. By contrast the differences for pure Ir are only 0.05 eV and 0.23 eV as we saw above.

GGA BAND STRUCTURE OF $(\mathrm{Cu-Os})$/GRAPHENE AND $(\mathrm{Cu-Ir})$/GRAPHENE

The electronic properties of (Cu-Os)/graphene and (Cu-Ir)/graphene are insensitive to the gradient correction in the exchange-correlation functional. Our GGA calculations (including spin-orbit coupling) yield the band structures shown in Fig. 5 and predict that both systems are non-magnetic. The topological insulator gaps evident in the figure are 0.21 eV for (Cu-Os)/graphene and 0.25 eV for (Cu-Ir)/graphene. All of these results agree well with our findings based on LDA.

It should be pointed out that electronic properties of Os/graphene and Ir/graphene *do* depend on the choice of exchange-correlation functional. Based on GGA calculations using the all-electron full-potential linearized augmented plane (FLAPW) method [7], Zhang *et al*. reported two gaps for Os/graphene with magnitude 11 meV (at 0.15 eV above the Fermi level) and 80 meV (at 0.38 eV below the Fermi level) [5]. Note that these gaps do not correspond to topological insulator phases, but rather quantum anomalous Hall states due to large moments predicted by GGA with or without spin-orbit coupling [5]. Our GGA calculations reproduced similar features, though the gap sizes are smaller: 3 meV and 40 meV.

It is thus important to deduce whether GGA or LDA is more appropriate for describing Os and Ir on graphene. The ultimate answer to the question must of course come from experiment. There is, however, reason to expect LDA to be more reliable here. For example, GGA has been found to yield unreliable results for $5d$ elements in low dimensions [8] as well as the description of the interaction between graphene and an Ir(111) surface [9]. Therefore we focused on LDA results for all cases in the main text.

* aliceaj@caltech.edu
† wur@uci.edu

[1] L. Fu and C. L. Kane, Phys. Rev. B **76**, 045302 (2007).
[2] P. E. Blochl, Phys. Rev. B **50**, 17953 (1994).
[3] G. Kresse and D. Joubert, Phys. Rev. B **59**, 1758 (1999).
[4] H. J. Monkhorst and J. D. Pack, Phys. Rev. B **13**, 5188 (1976).
[5] H. Zhang, C. Lazo, S. Blügel, S. Heinze, and Y. Mokrousov, Phys. Rev. Lett. **108**, 056802 (2012).
[6] C. Weeks, J. Hu, J. Alicea, M. Franz, and R. Wu, Phys. Rev. X **1**, 021001 (2011).
[7] E. Wimmer, H. Krakauer, M. Weinert, and A. J. Freeman, Phys. Rev. B 24, 864 (1981); M. Weinert, E. Wimmer, and A. J. Freeman, ibid. 26, 4571 (1982); M. Weinert, J. Math. Phys. (NY) 22, 2433 (1981).
[8] P. van Beurden and G. J. Kramer, Phys. Rev. B **63**, 165106

(2001).
[9] R. Brako, D. Šokčević, P. Lazić, and N. Atodiresei, New J. Phys. **12**, 113016 (2010).